INTERIM REPORT

Bulk Magnetization Effects in EMI-Based Classification and Discrimination

SERDP Project MR-1711

APRIL 2012

Thomas Bell
SAIC

This document has been cleared for public release

SERDP
DOD ▪ EPA ▪ DOE

This report was prepared under contract to the Department of Defense Strategic Environmental Research and Development Program (SERDP). The publication of this report does not indicate endorsement by the Department of Defense, nor should the contents be construed as reflecting the official policy or position of the Department of Defense. Reference herein to any specific commercial product, process, or service by trade name, trademark, manufacturer, or otherwise, does not necessarily constitute or imply its endorsement, recommendation, or favoring by the Department of Defense.

Abstract

The goal of this research project is to develop improved capabilities for classifying buried objects as unexploded ordnance (UXO) or clutter that exploit all of the information available in the electromagnetic induction (EMI) response of the object. There are two basic components in the EMI response: magnetization of the object by the primary field and the evolution of eddy currents set up in the object by changes in the primary field. The first is accessible only with sensors which measure the secondary (induced) response while the primary field is present (on-time response). Such sensors must null out the direct effect of the primary field on the receiver in order to see the much weaker secondary field. Current sensor systems used for classification are transient or time domain EMI (TEM) systems which measure the response after the primary field is shut off. They only measure the eddy current response.

The technical objectives for the initial phase of this project are to (1) establish, through analysis and supporting measurements, what the bulk magnetization response adds to classification performance and (2) develop a comprehensive understanding of the engineering challenges of primary field cancellation that can support a rational evaluation of whether or not it is possible to build an instrument that can reliably access both the bulk magnetization response and the eddy current response.

This report documents our findings relative to the first of the technical objectives. We used a lab bench setup to measure the on-time response of clutter items that were misclassified as munitions in recent ESTCP classification demonstrations. We find that the demagnetizing factors which characterize the bulk magnetization response do indeed convey information that is useful for distinguishing between smaller munitions items (20 mm, 37 mm etc.) and fragments of exploded larger caliber munitions whose TEM signatures are similar. Most of the misclassified clutter in the demonstrations at former Camp Butner and former Camp Beale could be correctly classified with a sensor that measured the bulk magnetization response in addition to the traditional eddy current response. It is likely that at least some of these items could be correctly classified with a time domain sensor capable of measuring very early time (order 10 μs) response. However, that would also require some form of primary field shielding or cancellation. Current TEM sensors remain seriously affected by primary field artifacts out to 100 μs and beyond.

A companion report documents our findings on the second objective. We conclude that a partial Helmholtz bucking coil configuration should provide adequate primary field cancellation and drift stability to enable reliable measurement of the complete EMI response. Based on these findings we recommend that the project proceed with development of a prototype sensor and further study of the significance of the bulk magnetization and very early time eddy current response for UXO/clutter classification and discrimination.

Table of Contents

Abstract i
Table of Contents ii
List of Tables ii
List of Figures iii
List of Acronyms iv
Keywords v
Acknowledgements vi
Objective 1
Background 2
  Introduction 2
  TEM Classification Performance 2
  Bulk Magnetization 3
Materials and Methods 5
  UXO-like Clutter 5
  FDEM Measurements 8
  Demagnetizing Factors 8
Results and Discussion 10
Conclusions and Implications for Future Research/Implementation 16
Literature Cited 17

List of Tables

Table 1. Munitions types for UXO-like clutter items. 5
Table 2. Repeatability test: 24 measurement sequences with 20 mm M51A projectile. 9
Table 3. Axial and transverse response time scales for small munitions items. 13

List of Figures

Figure 1. Receiver Operating Characteristic summarizing classification performance of the man-portable TEMTADS array at the former Camp Beale demonstration. 3
Figure 2. . Schematic illustration of magnetization and the demagnetizing field. In (a) the object is in its unmagnetized state. (b) shows the effects of an applied magnetic field H_0. The little bars represent magnetic domains and H_d is the demagnetizing field due to the aligned magnetic domains. 4
Figure 3. Size distribution of exploded ordnance fragments at the former Camp Beale demonstration. 6
Figure 4. Distributions of asymmetry factor (fractional difference between secondary polarizabilities) for intact munitions and munitions fragments at former Camp Beale. 6
Figure 5. Principal axis polarizabilities for 37 mm projectiles at the former Camp Butner demonstration, calculated using field data (top) and from test stand measurements (bottom). 7
Figure 6. Experimental setup for FDEM measurements. 8
Figure 7. Frequency domain EM response of a 57 mm projectile oriented with axis perpendicular to the primary field. 9
Figure 8. Demagnetizing factors and FDEM response time scales for munitions items and munitions-like clutter items. Different colors identify principal axes of clutter items. 10
Figure 9. Measured demagnetizing factors compared with calculated demagnetizing factors for ellipsoids and rectangular prisms having the same nominal dimensions. 11
Figure 10. Demagnetizing factor distributions for 20mm-like frag and 20 mm projectiles recovered from an impact area at Jefferson Proving Ground. 12
Figure 11. 20 mm rounds corresponding to EMI response data in Figure 10. 13
Figure 12. TEM coil ring-down after primary field cut-off. 14

List of Acronyms

EMI	Electromagnetic Induction
ESTCP	Environmental Security Technology Certification Program
FDEM	Frequency Domain EMI
GEM	Geophex Electromagnetic
GEMTADS	GEM MTADS
HE	High Energy Explosive
MR	Munitions Response
MTADS	Multisensor Towed Array Detection System
NRL	U.S. Naval Research Laboratory
ROC	Receiver Operating Characteristic
SAIC	Science Applications International Corporation
SERDP	Strategic Environmental Research and Development Program
TEM	Transient (time domain) EMI
TEMTADS	Transient Electromagnetic MTADS
UXO	Unexploded Ordnance

Keywords

electromagnetic induction, EMI, FDEM, TEM, demagnetizing factor, eddy current, munitions, clutter, classification, magnetic polarizability, UXO, munitions response

Acknowledgements

This project is a collaborative effort with contributions from Science Applications International Corporation (SAIC), Nova Research and G&G Sciences. Daniel Steinhurst of Nova Research and David George of G&G Sciences are co-principal investigators. The use of the Naval Research Laboratory's EMI sensors and their Blossom Point facility for test data collection is gratefully acknowledged. The work is supported by the Strategic Environmental Research and Development Program.

Objective

The objective of this research project is to develop improved capabilities for classifying buried objects as unexploded ordnance (UXO) or clutter that exploit all of the information available in the electromagnetic induction (EMI) response of the object.

There are two basic components in the EMI response: magnetization of the object by the primary field and the evolution of eddy currents set up in the object by changes in the primary field. Current sensor systems used for classification only measure the eddy current response. The technical objectives for the initial phase of this project are to (1) establish, through analysis and supporting measurements, what the bulk magnetization response adds to classification performance and (2) develop a comprehensive understanding of the engineering challenges of primary field cancellation that can support a rational evaluation of whether or not it is possible to build an instrument that can reliably access both the bulk magnetization response and the eddy current response. This information will be used evaluate whether or not the project should proceed to develop and test a prototype sensor capable of measuring both the bulk magnetization and eddy current responses.

This report documents our findings relative to the first of the technical objectives. We conclude that measuring the bulk magnetization response would allow clutter targets that are being misclassified as munitions with the current sensors to be properly classified as clutter. It is likely that at least some of these items could be correctly classified with a time domain sensor capable of measuring very early time (order 10 μs) response. However, that would also require some form of primary field shielding or cancellation. Current TEM sensors remain seriously affected by primary field artifacts out to 100 μs and beyond.

A companion report [1] documents our findings on the second objective. We conclude that a partial Helmholtz bucking coil configuration should provide adequate primary field cancellation and drift stability to enable reliable measurement of the complete EMI response. Based on these findings we recommend that the project proceed with development of a prototype sensor and further study of the significance of the bulk magnetization and very early time eddy current response (accessible only with primary field screening or cancellation) for UXO/clutter classification and discrimination.

Background

Introduction

One of the goals of current research and development activity in SERDP's Munitions Response focus area is developing effective technologies for classifying buried objects as munitions or clutter. That research has shown that EMI sensors offer the greatest potential for effective classification. There are two basic components in the EMI response to munitions and clutter items: magnetization of the object by the primary field and the evolution of eddy currents set up in the object by changes in the primary field. Most research activity has focused on the latter, leading to the development of sophisticated time domain or transient EMI (TEM) sensor systems which accurately measure the eddy current response following a transmitted primary field pulse. Although these sensors have proven to be quite effective in classifying buried objects, they do not exploit all of the information that is available in the EMI response, and they do misclassify some targets. We are interested in determining the extent to which classification performance can be improved with sensors that exploit the information available in both the bulk magnetization and the eddy current components of the EMI response.

Our analysis is based on classification performance with the TEM variants of the Multisensor Towed Array Detection System (MTADS) developed by U.S. Naval Research Laboratory (NRL). There are three versions: a vehicle towed 5x5 array and a man-portable 2x2 array and a single element handheld sensor. They are collectively referred to as the TEMTADS family.

TEM Classification Performance

TEM classification is based on principal axis polarizabilities calculated by dipole inversion of data collected over the target [2, 3]. The polarizabilities correspond to the eddy current responses to unit strength excitation along the target's three principal axis directions, and completely describe that part of the target's EMI response due to eddy currents. Targets are classified by comparing their polarizabilities against those of targets of interest and training data for the site.

The Receiver Operating Characteristic (ROC) shown in Figure 1 summarizes the classification performance of the man-portable TEMTADS array [4] at the former Camp Beale demonstration in the summer of 2011. The red portion of the curve corresponds to targets which were classified as munitions. No munitions items were misclassified. About fifty clutter items were misclassified as munitions, and over ninety percent of these were fragments of exploded large caliber munitions. Similar results hold for the full vehicle-towed TEMTADS array [5] at the former Camp Butner demonstration in 2010 and for the other TEM systems used at the various ESTCP live-site demonstrations. The question is whether or not the additional information available in the bulk magnetization response of these misclassified munitions fragments would allow us to properly classify them.

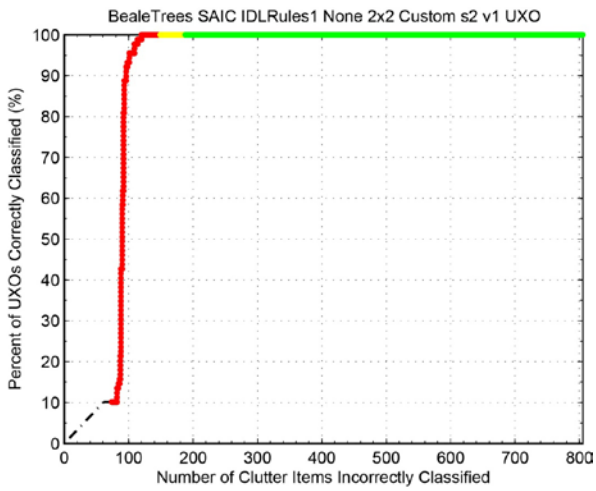

Figure 1. Receiver Operating Characteristic summarizing classification performance of the man-portable TEMTADS array at the former Camp Beale demonstration.

Bulk Magnetization

The effects of magnetization are illustrated schematically in Figure 2. The picture on the left (a) shows an object in its unmagnetized state. The little bars represent randomly oriented magnetic domains. When a magnetic field (H_0) is applied to the object (b), the magnetic domains distort and rotate towards alignment with the applied field and the object becomes magnetized. The intensity of magnetization is $M = (\mu\text{-}1)H_0$, where μ is the magnetic permeability of the object. The magnetic induction is $B = M + H_0 = \mu H_0$. The alignment of the magnetic domains results in a buildup of opposite magnetic poles on either side of the object, which creates a demagnetizing field H_d in opposition to the applied field and the magnetization. It is proportional to the magnetization ($H_d = \nu M$), and the constant of proportionality ν is called the demagnetizing factor [6]. For a very thin piece of steel with the applied field perpendicular to its surface, the accumulated poles on either side are close to each other and $\nu \rightarrow 1$. It is not just the thinness of the material, but also the object's overall shape that matters here. This is because the object tends to draw in the magnetic field lines. Only when the object's width is much larger than its thickness does $\nu \rightarrow 1$. For a long rod with a parallel applied field, the accumulated poles at either end are far apart, and $\nu \rightarrow 0$. Most munitions items are basically steel cylinders with about 4:1 length to diameter aspect ratio, with demagnetizing factors $\nu \sim 0.1$ for an axial applied field, and $\nu \sim 0.4$ for a transverse field [7].

Fragments of exploded ordnance items tend to be kind of jagged and less regular than intact ordnance items. At issue is whether or not this affects the demagnetizing factors in such a way that the complete EMI responses of intact munitions items and comparably sized munitions fragments can be reliably distinguished.

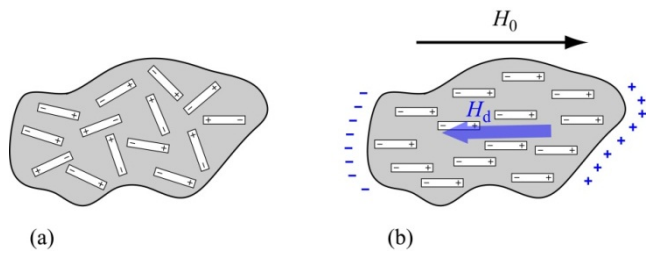

Figure 2. . Schematic illustration of magnetization and the demagnetizing field. In (a) the object is in its unmagnetized state. (b) shows the effects of an applied magnetic field H_0. The little bars represent magnetic domains and H_d is the demagnetizing field due to the aligned magnetic domains.

The target is magnetized only while the primary field is on (i.e., during the on time), hence the target's magnetization response is only present while the primary field is present. Traditional time domain EM sensors don't try to capture the on-time response, but rather shut off the primary field and then watch the decaying eddy current signals. If we use a continuously varying primary field, the target's magnetization varies continuously with the changing primary field, and eddy currents are continuously swirling about and changing in response to the primary field. With simple frequency domain EMI (FDEM) sensors, the magnetization response shows up as an offset of the response in phase with the primary field. The eddy current response varies with frequency and is phase shifted relative to the primary field. Secondary fields due to the induced magnetization and eddy currents are overwhelmed by the primary field at the receiver. The primary field has to be cancelled or nulled out in order to be able to measure the induced field component in phase with the primary. This problem is addressed in our companion report [1].

Materials and Methods

UXO-like Clutter

152 clutter items which were misclassified as munitions in the ESTCP classification demonstrations at former Camp Butner in 2010 and former Camp Beale in 2011 were identified for analysis. The Camp Butner demo used the 5x5 TEMTADS array [5] and the Camp Beale demo used the 2x2 man-portable TEMTADS [4]. Of these 152 UXO-like clutter items, 87 were from Camp Butner and 67 from Camp Beale. Some of these items were included as training data and do not show up as misclassified clutter in the body of the ROC. The corresponding "apparent" munitions types are listed in Table 1. The counts illustrate that misclassified clutter is primarily a problem for sites with smaller munitions items. Mostly we are dealing with fragments of exploded larger high energy explosive (HE) filled munitions. There are a lot of finger-sized fragments which can look like 20 mm projectiles to the TEM sensors. There tend to be fewer that can be confused with 37 mm projectiles, and very few that can be confused with larger munitions. The point is illustrated by Figure 3, which shows the size distribution of exploded ordnance fragments at the former Camp Beale demonstration. The apparent size is proportional to the cube root of the object's net polarizability determined from the TEM array measurement over the object. Very small sizes are under-represented in the plot because they tend to have EMI signals below the anomaly selection threshold for the demonstration. The frag size distribution for former Camp Butner is similar. Most of the frag was likely from exploded 105 mm projectiles. Larger frag was recovered at the 1999 MTADS demonstration at the Badlands Bombing Range, SD impact area, along with eight live 155 mm and seven live 8 inch projectiles [8].

Type	Number
20 mm	199
37 mm	24
60 mm	1
81 mm	1
105 HEAT	1
ISO	6

Table 1. Munitions types for UXO-like clutter items.

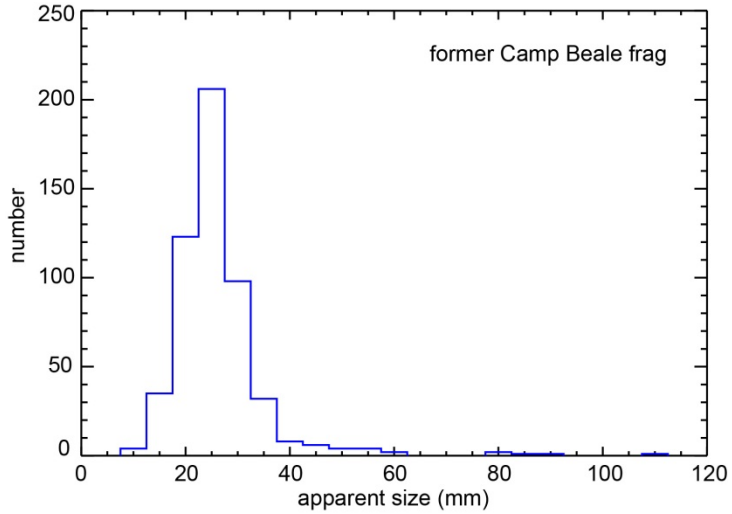

Figure 3. Size distribution of exploded ordnance fragments at the former Camp Beale demonstration.

By and large, for a clutter item to be misclassified as UXO it is necessary, but not sufficient that the item appear to be axially symmetric. Figure 4 shows distributions of the EMI signature asymmetry factor (fractional difference between secondary polarizabilities) for all munitions fragments (right scale) and for UXO and UXO-like frag (left scale) at former Camp Beale. Outliers (large asymmetry factor) in the latter two distributions are associated with noise contamination and/or inversion problems for targets having weak signals. The distributions show that because we have to accommodate such effects we tend to be a bit conservative in our classification procedures. Targets with secondary polarizabilities that are slightly different are still likely to be classified as munitions if the amplitudes and shapes of their polarizabilities are a reasonable match to those of a target of interest.

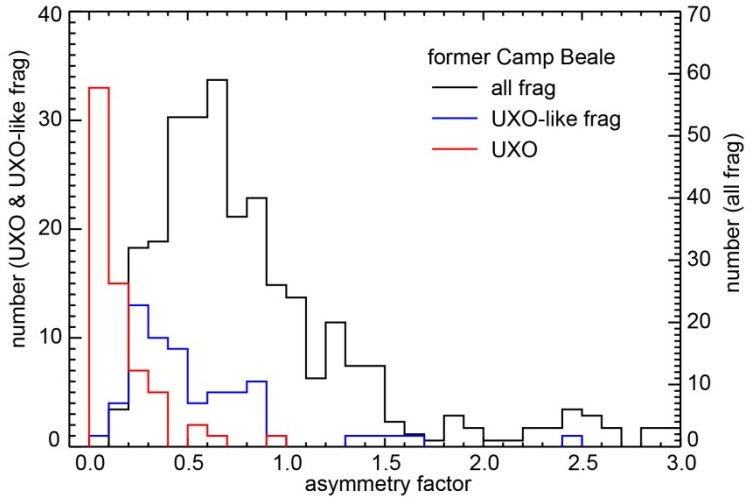

Figure 4. Distributions of asymmetry factor (fractional difference between secondary polarizabilities) for intact munitions and munitions fragments at former Camp Beale.

Figure 5 gives some idea of the tolerance that has to be allowed in matching an unknown target's EMI signature to the signatures of targets of interest. The top plot shows principal axis polarizabilities calculated using the field data collected over all of the 37 mm targets at the former Camp Butner demonstration. The bottom plot shows corresponding polarizabilities calculated using test stand measurements of the recovered 37 mm targets back at the Naval Research Lab's Blossom Point facility. Although the test stand data tighten up the spread in the field polarizabilities there is still signature variability. One can distinguish several distinct groups of curves in the test results which correspond to different types of 37 mm projectile. Those with the strongest polarizability at the earliest times are projectile bodies missing the rotating band. The rotating band is typically a copper alloy swaged into a circumferential groove near the aft end of the steel projectile body, and can be damaged or break off on impact.

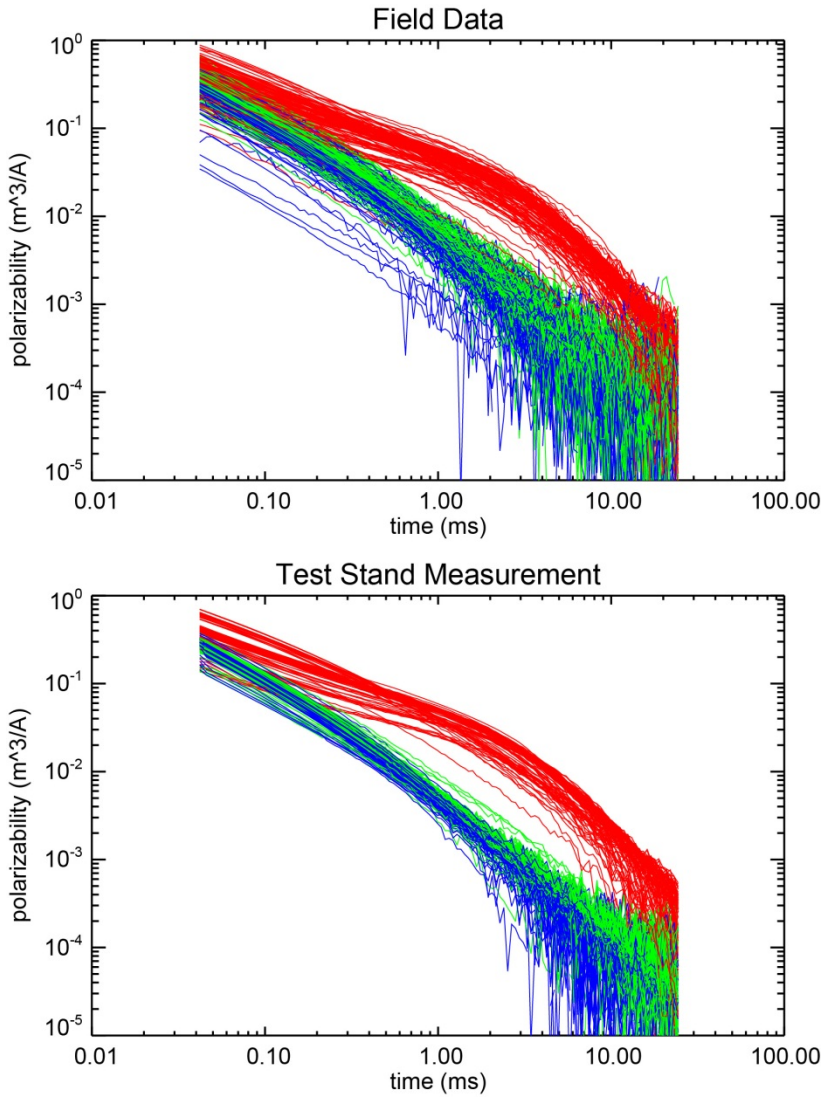

Figure 5. Principal axis polarizabilities for 37 mm projectiles at the former Camp Butner demonstration, calculated using field data (top) and from test stand measurements (bottom).

FDEM Measurements

We measured the FDEM response of the UXO-like clutter using a Geophex GEM-3 sensor [9]. Figure 6 shows the experimental setup. For each measurement the item was centered on the axis of the GEM coil at a distance of ~25 cm from the coil (a). Munitions items were measured with the nose pointing towards the coil (0°) and at 90°, 180° and 270° rotations. Frag items typically have one side flatter than the others. Each was measured at 0°, 90°, 180° and 270° with the flat side down (b) then rotated 90° about the long axis so that it was on edge (c) and measured at the 0°, 90°, 180° and 270° angle sequence. Background shots were taken before and after and in between measurements and interpolated to the actual measurement times to control drift. We used a ferrite rod to check and level the GEM's frequency response. Data were collected at 0.15, 0.27, 0.57, 1.23, 2.61, 5.43 and 11.43 kHz. Data at higher or lower frequencies were not reliable because of drift and noise problems with the GEM.

Figure 6. Experimental setup for FDEM measurements.

Controlled in-air measurements of the TEM responses of these objects were made with the manportable TEMTADS array. As might be expected in light of the results shown in Figure 5, some of the items that appeared UXO-like in the field data did not have UXO-like in-air signatures. These items were not included in our analysis.

Demagnetizing Factors

Demagnetizing factors were calculated from the measured FDEM response by fitting the data with our standard FDEM response model [10]

$$S(\omega) = a_0 + a_1 \frac{(i\omega\tau)^\gamma - 2}{(i\omega\tau)^\gamma + 1}.$$

Figure 7 illustrates how this works. It shows the response for a 57 mm projectile, one of the SERDP project MR-1313 [11] munitions items. The symbols show the response measured with a GEM-3 sensor, blue diamonds for the component in phase with the primary field and red triangles for the component in quadrature (90° out of phase). The projectile was 39 cm from the sensor, aligned perpendicular to the primary field direction. The curves show our fit to the

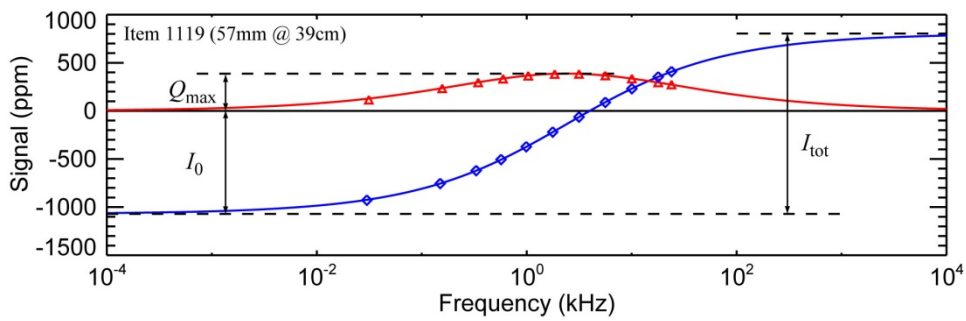

Figure 7. Frequency domain EM response of a 57 mm projectile oriented with axis perpendicular to the primary field.

measured signal. The magnetization of the projectile produces the in phase offset I_0. If the target were non-magnetic, I_0 would be zero. The demagnetizing field (H_d) shifts the in phase response curve upwards. When $\nu \to 1$, $H_d \to M$ and the demagnetizing field cancels the effect of the magnetization response. In this event the object behaves like it is nonmagnetic and the curve shifts up so that $I_0 \sim 0$. When $\nu \to 0$, the demagnetizing field is inconsequential, and the in phase response is shifted down so that $I_0 \sim I_{tot}$. In general, the demagnetizing factor is given by

$$\nu = \lim_{\omega \to \infty} \frac{S(\omega)}{S(\omega) - S(0)} = 1 - \frac{I_0}{I_{tot}}.$$

which can be calculated directly from the model fit to the data. This procedure has been shown to produce good results for munitions sized objects [2].

We checked the repeatability of the measurements using the 20 mm M51A projectile shown on the stand in Figure 6a. This was the library item that was most frequently identified with UXO-like clutter. We repeated the measurement cycle 24 times with slight variations (6-7 mm) in the distance from the coil. The results are shown in Table 2. Measurement errors are about ½-1%.

Configuration	Demagnetizing Factor	
	mean	std. dev.
Nose towards coil (0°)	0.07030	0.00065
Nose to right (90°)	0.42335	0.00289
Base towards coil (180°)	0.07715	0.00080
Nose to left (270°)	0.42220	0.00285

Table 2. Repeatability test: 24 measurement sequences with 20 mm M51A projectile.

Results and Discussion

We were able to recover and measure 43 of the items from Table 1. Of these, 39 had UXO-like TEM signatures when measured on a test stand with the man-portable TEMTADS array. These were measured with the GEM. The 105 HEAT match turned out to be a rolled up slab of steel and was not measured with the GEM. The 81 mm match is an enigma. The recovered object for that target was much too small to produce the response measured over the anomaly. It was not measured with the GEM either.

The processed results for the 39 UXO-like clutter items are shown in Figure 8 as a scatter plot of demagnetizing factor ν vs. the characteristic response time scale τ. The response time scale τ is identified with the peak in the quadrature spectrum ($\tau = 1/\omega_p = 1/2\pi f_p$) and corresponds to the magnetic surface mode time scale in the TEM response [2]. Different colors (red, green, blue) are used to identify responses along the three principal axis directions of the frag items. Red corresponds to the long axis. Blue corresponds to the direction perpendicular to the "flat" face (up in Figure 6b) and green to the remaining direction (up in Figure 6c). Recall that the responses were measured with the target's principal axis aligned both parallel to and anti-parallel to the GEM coil axis, so there are 78 data points per axis. Processed results for the measured responses of the corresponding 20 mm and two 37 mm (one longer, one shorter) library matches are shown using the black symbols.

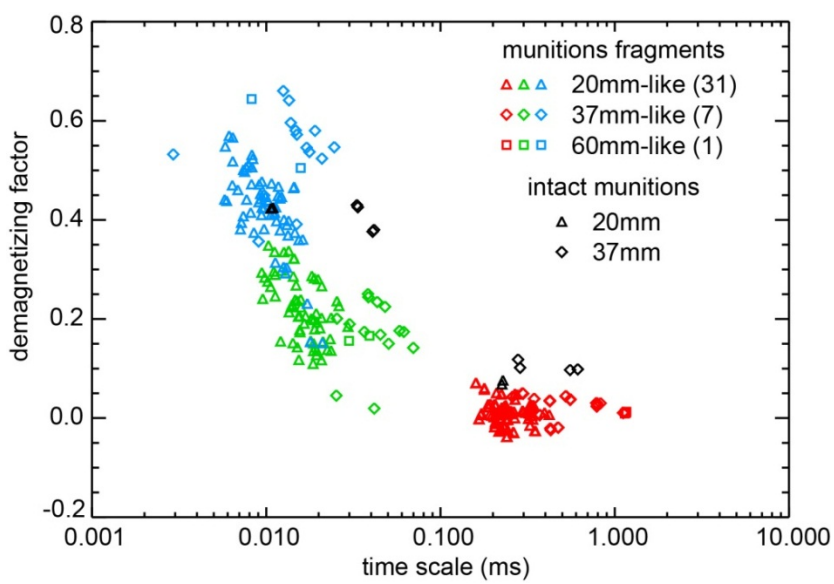

Figure 8. Demagnetizing factors and FDEM response time scales for munitions items and munitions-like clutter items. Different colors identify principal axes of clutter items.

For fixed object size, ν and τ are correlated. The response time scale depends on both the shape and the size of an object. It is larger when a UXO-like object is excited along its long axis that it is when excited in the transverse direction by an amount that depends on the length to diameter

aspect ratio, and it increases as the square of the object's size [12]. The demagnetizing factor depends on the shape, but not the size of an object. It is smallest in the direction of the longest dimension and largest in the direction of the shortest dimension. The three principal axis demagnetizing factors sum to one for a uniformly magnetized object, but typically only spheres and ellipsoids will be uniformly magnetized.

Secondary axis demagnetizing factors (blue and green) for the frag tend to spread out into clouds which seem to amplify the differences between the secondary axis dimensions (average dimensions for the 20mm-like frag are 9.18, 2.36 and 1.42 cm). Also, everything is shifted down relative to the demagnetizing factors for the corresponding munitions items. We attribute this to the jagged nature of shattered steel fragments. The effect is illustrated in Figure 9, which compares the measured demagnetizing factors with demagnetizing factors calculated for ellipsoids [13] and uniformly magnetized rectangular blocks or prisms [14] having the same nominal dimensions as the various items. Measured demagnetizing factors for the intact munitions items are comparable to the demagnetizing factors for similar ellipsoids and prisms. The demagnetizing factors for the munitions fragments tend to be significantly reduced relative to those for smooth, solid objects having the same nominal dimensions. This trend is consistent with the expected contributions to the demagnetizing factor from the points and cusps on the jagged edges of exploded munitions fragments [15, 16].

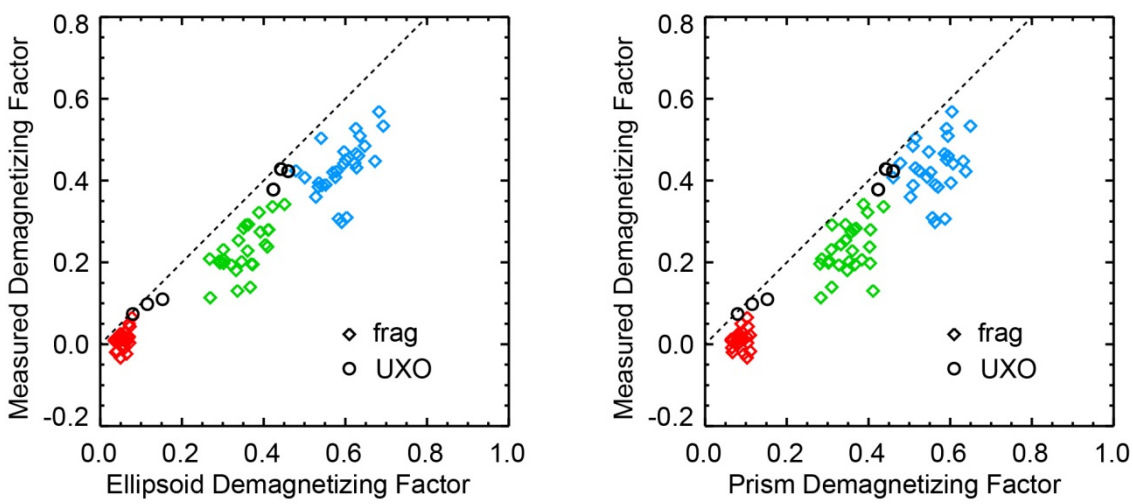

Figure 9. Measured demagnetizing factors compared with calculated demagnetizing factors for ellipsoids and rectangular prisms having the same nominal dimensions.

Real UXO recovered from firing ranges are often dented, bent, broken, or otherwise damaged. This introduces variability in the EMI responses of nominally the same objects. Figure 5 showed the TEM response variability of 37 mm projectiles at the former Camp Butner demonstration. Figure 10 compares the FDEM response variability of a dozen 20 mm rounds recovered from an impact area at Jefferson Proving Ground with the 20mm-like frag from Figure 8. The 20 mm

rounds (shown in Figure 11) were measured with the GEM-3 in SERDP project MR-1313 [11]. The set includes partial rounds and rounds with broken or missing rotating bands. The 20 mm projectile responses group more tightly than the 20mm-like frag responses. The frag items are not cylindrical, so they have two distinct secondary axis responses (blue and green). The spread out intermediate axis response (green) that is present for the frag would be missing for the 20 mm rounds. The 20 mm axial time scales split into one of two groups depending on whether or not the rotating band is intact, but a similar effect is not seen in the corresponding demagnetizing factors.

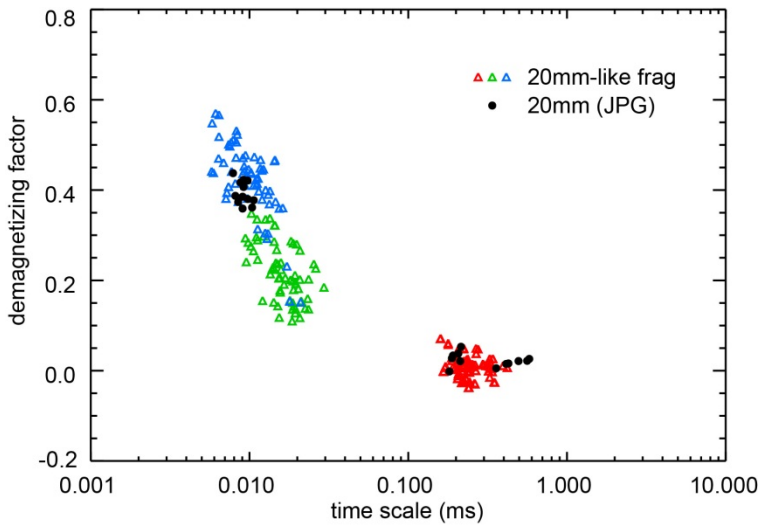

Figure 10. Demagnetizing factor distributions for 20mm-like frag and 20 mm projectiles recovered from an impact area at Jefferson Proving Ground.

The demagnetizing factors convey EMI response information that is useful for distinguishing between smaller munitions items (viz. 20 mm and 37 mm) and fragments of exploded larger caliber munitions whose TEM signatures are similar. Most of the misclassified clutter in the demonstrations at former Camp Butner and former Camp Beale could likely be correctly classified if this information were included.

Since the demagnetizing factors and response time scales in Figure 8 (or Figure 10) are correlated it seems possible that a TEM estimate of τ would be just as effective for classification as a FDEM estimate of ν. Unfortunately, the transverse response time scales are difficult to resolve with existing TEM sensors. In the time domain τ marks a very broad and gradual inflection as the TEM response decay rate transitions from $t^{-1/2}$ to $t^{-3/2}$ behavior [2, 3]. For smaller munitions items transversely excited this occurs at very early times (of order 10 μs). Values determined from the FDEM response of various fired/recovered small caliber munitions items measured for SERDP project MR-1313 [11] are listed in Table 3.

Figure 11. 20 mm rounds corresponding to EMI response data in Figure 10.

At these early times the response of standard TEM sensors is still dominated by saturation and ring-down of the receive coils after the primary field cutoff. Figure 12 shows the early time background (no target) response of the various TEMTADS coils. The response is actually saturated out to about 10 μs. Beyond that out to about 100 μs the response is significantly affected by ring-down variations associated with temperature and other environmental effects on the coils and electronics. In order to reliably measure target response at very early times some form of primary field cancellation or shielding would be needed, which is what we are trying to do in this project anyway.

Type	Characteristic Time Scale (ms)			
	axial		transverse	
	mean	std. dev.	mean	std. dev.
20 mm A*	0.254	0.160	0.0086	0.0012
20 mm B	0.634	0.027	0.0150	0.0010
25 mm	0.691	0.022	0.0279	0.0012
37 mmA	2.419	0.834	0.0340	0.0041
37 mm B	2.745	0.315	0.0391	0.0052
37 mm C*	0.542	0.085	0.0313	0.0031

*rotating band broken

Table 3. Axial and transverse response time scales for small munitions items.

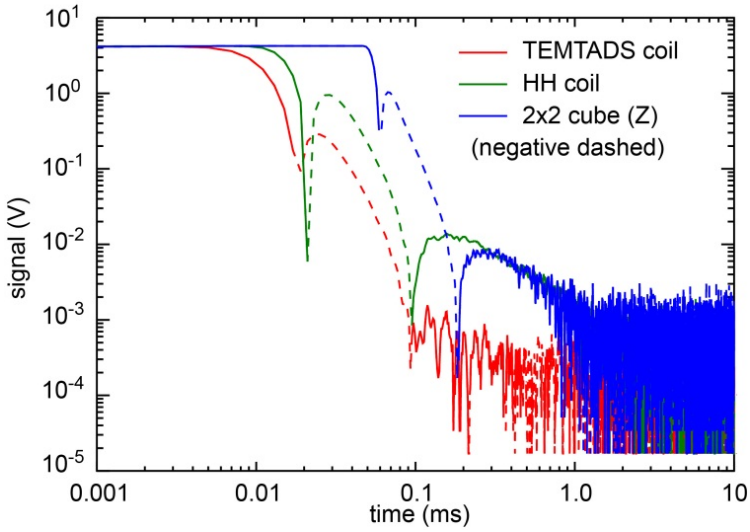

Figure 12. TEM coil ring-down after primary field cut-off.

The correlation between ν and τ and its potential implications were noted in SERDP project MR-1315. That project was the precursor to the development of the TEMTADS system, and its basic conclusion was:

> "Although all our results lead us to believe that in the high signal-to-noise case the best choice for discrimination would be a frequency-domain sensor, this program is concerned with a survey instrument rather than a cued detection instrument. For this reason, we have concluded during the past year that our prototype instrument will be a time-domain sensor." [17, p. 2]]

This decision was strongly influenced by the desire for a survey system and NRL's experience with the MTADS GEM-3 (GEMTADS) array [18] in surveys at the Yuma Proving Ground UXO Test Site, where significant in phase noise was caused by target scale variations in the soil response. If the in phase response could not be reliably used for target classification in a survey instrument, then the demagnetizing factors were not available and the primary motivation for a frequency domain sensor was removed. We are probably not talking about a survey instrument here. Current classification strategies call for a sensor array that can be used in survey mode to detect targets and classify the "easy" ones using the survey data, with the remainder classified later in cued mode [19]. What we are talking about here would most likely be used in the follow-up cued mode stage.

The original design spec for the TEMTADS sensors aimed for measuring the TEM response as early as 6 μs after primary field cutoff using a quadrupole (bucking) receiver coil. The mechanical alignment and adjustment required to maintain null coupling between the transmitter and receiver proved to be too hard and the concept was dropped in favor of traditional dipole receivers in TEMTADS as built [20]. The upshot is that current TEM sensors remain seriously

affected by primary field artifacts out to 100 μs and beyond. An earlier study [3] that looked at the former Camp Luis Obispo TEMTADS demonstration concluded that relaxing the early time cutoff from 40 μs to order 1 ms does not degrade classification performance. Of course that study used the current technology as a starting point, the smallest targets of interest were bazooka rockets, and there no the frag from larger HE filled projectiles. Munitions-like frag is fundamentally a small munitions problem, and with current technology the ability to correctly classify 20mm-like, 25mm-like, 30mm-like, 37mm-like and probably 40mm-like frag is already lost.

Conclusions and Implications for Future Research/Implementation

The demagnetizing factors which characterize the bulk magnetization response convey information that is useful for distinguishing between smaller munitions items (20 mm, 37 mm etc.) and fragments of exploded larger caliber munitions with similar TEM signatures. Most of the misclassified clutter in the ESTCP demonstrations at former Camp Butner and former Camp Beale would likely be correctly classified with a sensor that measured the bulk magnetization response in addition to the traditional eddy current response. Demagnetizing factors and magnetic surface mode time scales are correlated, so it is also likely that at least some of these items could be correctly classified with a time domain sensor capable of measuring the response at the very early times (order 10 μs) required to resolve the magnetic surface mode time scales for smaller munitions items. However, that would also require some form of primary field shielding or cancellation. Current TEM sensors remain seriously affected by primary field artifacts out to 100μs and beyond. Since munitions-like frag is fundamentally a small munitions problem, with current technology the ability to correctly classify 20mm-like, 25mm-like, 30mm-like, 37mm-like and probably 40mm-like frag is pretty much lost.

The engineering challenges of primary field cancellation are considered in a companion report [1]. We conclude that a partial Helmholtz bucking coil configuration should provide adequate primary field cancellation and drift stability to enable reliable measurement of the complete EMI response. Based on these findings we recommend that the project proceed with development of a prototype sensor and further study of the significance of the bulk magnetization and very early time eddy current response for UXO/clutter classification and discrimination.

Literature Cited

1. David George, "Design Study: An Electromagnetic Induction System for Observation of Bulk Magnetization Response of UXO Targets," Technical Report, SERDP Project MR-1711, May 2012.

2. Thomas Bell, "Phenomenology and Signal Processing for UXO/Clutter Discrimination," SERDP Project MR-1595 Final Report, August 2009.

3. Thomas Bell, "Magnetic Surface Modes and UXO/Clutter Classification and Discrimination," SERDP Project MR-1658 Final Report (draft), December 2011.

4. ESTCP Live Site Demonstrations, Former Camp Beale, Marysville, CA. Demonstration Plan Supplement: Former Camp Beale TEMTADS 2x2 Cart Survey (ESTCP project MR-1165), April 2011.

5. 2010 ESTCP UXO Classification Study Rougemont, NC. Demonstration Plan Supplement: Former Camp Butner MTADS Discrimination Array (TEMTADS) Survey (ESTCP project MR-1034), May 2010.

6. Richard M. Bozorth, Ferromagnetism, Wiley-IEEE Press, Hoboken, 1993. R. Moskowitz and E. Della Torre, "Theoretical Aspects of Demagnetization Tensors," IEEE Trans. Magnetics, vol. 2, no. 4, pp. 739-744, December 1966.

7. Du-Xing Chen, James A. Brug and Ronald B. Goldfarb, "Demagnetizing Factors for Cylinders," IEEE Trans. Magnetics, vol. 37, no. 4, pp. 3601-3619, July 1991.

8. J.R. McDonald, H.H. Nelson, R. Robertson and R.A. Jeffries, “MTADS Unexploded Ordnance Operations at the Badlands Bombing Range, Air Force Retained Area,” Naval Research Laboratory Report NRL/PU/6110-00-424, September 1999.

9. I.J. Won, Dean A. Keiswetter, David R. Hanson, Elena Novikova and Thomas M. Hall, "GEM-3: A Monostatic Broadband Electromagnetic Induction Sensor," Journal of Environmental and Engineering Geophysics, vol. 2, no. 1, pp. 53-64, March 1997.

10. Jonathan T. Miller, Thomas H. Bell, Judy Soukup and Dean Keiswetter, "Simple Phenomenological Models for Wideband Frequency-Domain Electromagnetic Induction," IEEE Trans. Geoscience and Remote Sensing, vol. 39, no. 6, pp. 1294-1298, June 2001.

11. Jonathan Miller, "Quantification of UXO Variability for Target Discrimination," Final Report SERDP Project MR-1313, April 2007.

12. Thomas Bell, Bruce Barrow, Jonathan Miller and Dean Keiswetter, "Time and Frequency Domain Electromagnetic Induction Signatures of Unexploded Ordnance," Subsurface Sensing Technologies and Applications, vol. 2, no. 3, pp. 153-175, July 2001.

13. J.A. Osborn, “Demagnetizing Factors of the General Ellipsoid,” Physical Review, Vol. 67, No. 11/12, June 1945, pp. 351-357.

14. Amikam Aharoni, "Demagnetizing factors for rectangular ferromagnetic prisms," J. Applied Physics, Vol. 83, No. 6, March 1998, pp. 3432-3434.

15. Ken-ichi Ozaki and Masanori Kobayashi, "Surface Magnetic Charge Densities and Demagnetizing Factors for Rotating Astroids," IEEE Trans. Magnetics, Vol. 36, No. 1, January 2000, pp. 210-215.

16. Naoya Soda, Tatsuo Horii, and Masanori Kobayashi, "Magnetometric Demagnetizing Factors for Various Shapes of Rotational Symmetry," IEEE Trans. Magnetics, Vol. 45, NO. 12, December 2009, pp. 5289-5295.

17. "EMI Sensor Optimized for UXO Discrimination," SERDP Project MR-1315 Annual Report, January 2005.

18. "Enhanced UXO Discrimination Using Frequency-Domain Electromagnetic Induction," ESTCP Project MR-200033 Final Report, May 2007.

19. "ESTCP Munitions Responsee Live Site Demonstrations: Former Spencer Artillery Range, Tennessee," Demonstration Plan, March 2012.

20. D.A. Steinhurst, G.R. Harbaugh, J.B. Kingdon, T. Furuya, D.A. Keiswetter and D.C. George, "EMI Array for Cued UXO Discrimination," Final Report, ESTCP Project MM-0601, July 2010.